Reprinted from: OXYGEN TRANSPORT TO TISSUE
Instrumentation, Methods, and Physiology
Edited by Haim I. Bicher,
and Duane F. Bruley
Book available from: Plenum Publishing Corporation
227 West 17th Street, New York, N.Y. 10011

BASIC PRINCIPLES OF TISSUE OXYGEN DETERMINATION FROM MITOCHONDRIAL SIGNALS

B. Chance, N. Oshino, T. Sugano, and A. Mayevsky

Johnson Research Foundation, School of Medicine

University of Pennsylvania, Philadelphia PA 19104

The importance of measuring intracellular oxygen concentrations in tissues has, over the years, emerged as a basic parameter in the physiology and biochemistry of living tissues. The credibility of oxyhemoglobin determinations, even as refined A/V differences, is taxed especially in cases where inhomogeneous tissues with variable oxygen demands and oxygen supply are served. The formation of lactic acid in the venous blood is often used as a criterion of anoxia, but it also lacks credibility where inhomogeneous circulatory pathways are served and in addition, is questionable from the standpoint of whether the appearance of excess lactate is an unequivocal criterion of oxygen insufficiency. To indicate my empathy with polarographic techniques as they have been developed at the Johnson Foundation, I wish to recall the pioneering works of Bronk(1) Brink (2), Davies and Remond (3) that stand as landmarks in the exploration of tissue oxygen tension by microelectrode methods. I served my apprenticeship with them.

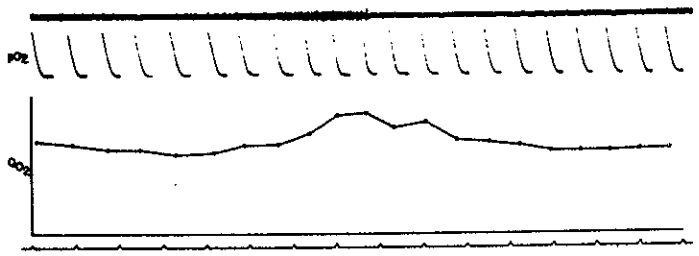

Figure 1. Illustrating the use of the platinum microelectrode to measure quantitatively the cortical oxygen tension during an epileptic seizure. Upper trace, electrocorticogram. Second, pO_2 shown as a series series of curves, each one giving oxygen tension as a function of time after local occlusion of the pial circulation. Third trace, Q_{O_2}, a plot of the linear portions of these curves as proportional to the rate of oxygen consumption. (From Davies & Remond, 1946 [3])

MITOCHONDRIAL INDICATION OF INTRACELLULAR pO_2

However, the organelles that surely exhibit the intracellular oxygen tension are the ones that are using the oxygen. These are the mitochondria. They do not need to be reached by electrodes; they emit spectroscopically detectable signals themselves. It is the purpose of this paper to show how these signals may be read.

The accumulation of evidence since the pioneer work of Otto Warburg on "atmungsferment"(4) and David Keilin on cytochromes (5) as the keystones of cellular oxygen utilization led us to a study of the redox states of electron carriers in isolated mitochondria as a function of oxygen concentration, and to develop techniques to measure the states of anoxia and normoxia in living tissues.

The morphology of the system is a primary consideration, and we shall begin by showing where the mitochondria are situated and what they may reveal on account of this location. The ubiquity of mitochondria in eukharyotic cells is due to their superlatively efficient energy conservation system. Often, one-third or more of the volume of an active tissue, such as mammalian cardiac tissue, may be filled with mitochondria. Similarly, the oxygen utilization of the brain as compared with that of the whole body stands as testimony to mitochondrial activity in that organ. Thus, there is no doubt that the readout of mitochondrial redox states takes us to the very source and furthermore, the cell membrane does not need to be penetrated in order to do so.

Granting that an intracellular indicator is thus available, the question remains as to how precisely it may be measured, i.e., how many mitochondria are required for a readable signal of their redox state? Fortunately, this has been determined by both microfluorometry and microspectrophotometry; using as experimental material a single large mitochondrion, that of the insect spermatid in meiotic telephase, we find signal-to-noise ratios of about 10 at bandwidths of a few cycles per sec(6,7). Somewhat improved performance has recently been obtained by the use of better light sources and photon-counting detectors. With lasers for light sources, even greater progress may be expected -- up to the point where photodestruction of the biological system could become highly significant. At least, one can say that a high signal-to-noise recording can be made from a tissue cross-section about one micron in diameter without penetrating the cell membrane.

Localization of the mitochondrial signal does not always require microscopic readout; one facet of localization that is not always appreciated emerges from a consideration of mitochondria in flight-muscle, where the repeat pattern of mitochondrial localization and function is sufficiently regular that averaging of the signal from many mitochondria nevertheless ensures that the recording can be referred to the intimate relationship of a single mitochondrion and its adjacent myofibril. It is not clear that this is the case with the brain, where the distribution of mitochondria in the cell bodies, the synapses, and the glia may well require microscopic techniques in order precisely to localize the mitochondrial response to a certain kind of process in a particular portion of a cell.

It is further appropriate to consider whether the mitochondrial redox state can be calibrated in terms of oxygen requirements. The oxygen requirements can be determined precisely by two general approaches, kinetic and steady-state. Considering first the kinetic method, we have a simple expression based on the assumption that the cytochrome oxidase system works on a mechanism that was demonstrated in detail in our early studies of peroxidase (8) according to modifications of the Michaelis-Menten theory:

$$K_m = k_3/k_1 \qquad (1)$$

The quantity k_3, while a kinetic parameter, is most readily determined from the steady state rate of oxygen utilization at high oxygen concentration, as measured by the oxygen electrode, and may simply be identified from the turnover number, TN, of cytochrome oxidase:

$$k_3 = TN = 4\,\frac{dO_2/dt}{[a_3]} \qquad (2)$$

The factor of 4 equates the number of oxidizing equivalents per mole of oxygen with the electron-handling capability of cytochrome a_3. Thus, K_m is directly proportional to the turnover number or the respiratory activity of the mitochondria.

The denominator of the expression, k_1, the rate of combination of cytochrome oxidase with oxygen, generally requires the use of the rapid flow apparatus for its determination. An example of the measurement of this constant by laser photolysis of CO-inhibited cytochrome oxidase in a suspension of isolated mitochondria in the presence of 17 μM oxygen is shown in Figure 2. It is seen that the reaction time is very short, about one millisecond under these particular conditions. This value, which is appropriate to the reaction of roughly 10 mm oxygen with the cytochrome oxidase of the tissue, is indeed the parameter to which cytochrome oxidase owes its remarkably high oxygen affinity. The value of K_m for several sources of resting mitochondria is calculated to be 10^{-8} M oxygen (9), and for highly activated mitochondria, about ten-fold greater, 3×10^{-7} M,

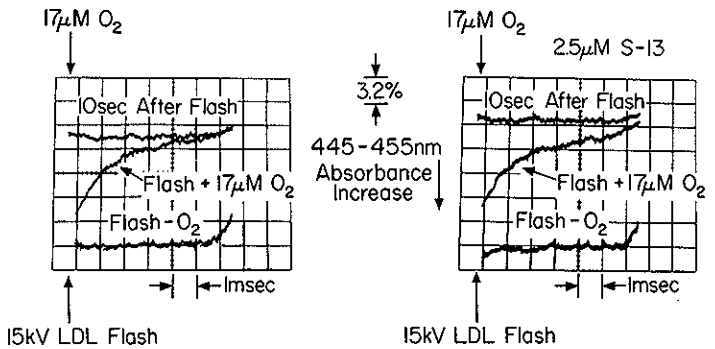

Figure 2. Illustrating the technique of laser flash photolysis for measuring the rate of reaction of oxygen (17 μM) with cytochrome oxidase in suspensions of CO-inhibited pigeon heart mitochondrial membranes in the coupled (left) and uncoupled (right) states. (127-8,9V; courtesy of Archives of Biochemistry and Biophysics [9]).

at 23°. The many identical properties of isolated and *in situ* mitochondria support the applicability of the *in vitro* data to the *in vivo* conditions.

The steady state approach has the advantage that it is strictly analogous to some of the procedures that are applicable to intact tissues as well. What is needed in this case is an extremely sensitive and linear oxygen indicator. A variety of approaches are available; we have preferred luminous bacteria (10) since they afford the greatest dynamic range, from almost 1 μM downwards towards 10^{-10} M. A calibration curve of the luminous bacteria system is shown in Figure 3 (11).

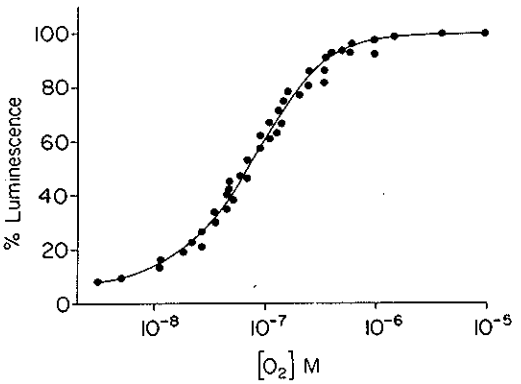

Figure 3. Calibration curve of oxygen consumption *vs.* luminescence in a suspension of *Achromobacter fischeri*. (NO-161)

The applicability of this method to the determination of the oxygen affinity of the cytochromes of pigeon heart mitochondria is illustrated in Figure 4, where p_{50} for cytochrome *c* has been evaluated. Plotted on a semilogarithmic scale, the cytochrome *c* response is sigmoidal, corresponding to a rectangular hyperbola. The oxygen concentration required for half-maximal oxidation of cytochrome *c* varies with the turnover number; 6×10^{-7} M oxygen for the

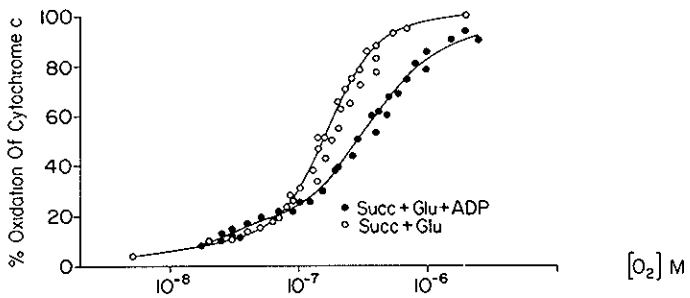

Figure 4. Semilogarithmic plot of cytochrome *c* oxidation as a function of oxygen concentration for the rapidly respiring State 3 (●) and without added ADP (○). (TS-N-5A)

rapidly respiring State 3 (12) in good agreement with the kinetic data. In the absence of ADP, a smaller K_m is observed but not as small as when the mitochondria are in a true resting State 4.

Relative Sensitivity to Anoxia of the Respiratory Components.

It is important to consider which component best represents the performance of the mitochondria. A synopsis of the components of the respiratory chain, roughly in order of increasing mid-potential, is shown in Figure 5. In an equilibrium system, the mid-potential of the respiratory components will determine their sensitivity to oxygen; the component at the most negative potential will respond most sensitively to oxygen, and that at the most positive potential, least sensitively. NADH, at approximately -300 mV, is at the extreme low potential end of the chain, and thus may be the oxygen indicator of choice in mitochondria and tissue as well; while one species of flavoprotein is also of a very negative mid-potential, the NADH fluorescence signal in the normoxic-anoxic transition is larger and less sensitive to artifacts. Cytochrome c, at +220 mV, is in the upper range of midpotentials and thus less sensitive to changes of oxygen concentration. From a kinetic standpoint, however, it is a more useful indicator of electron transport and energy coupling rates than is NADH.

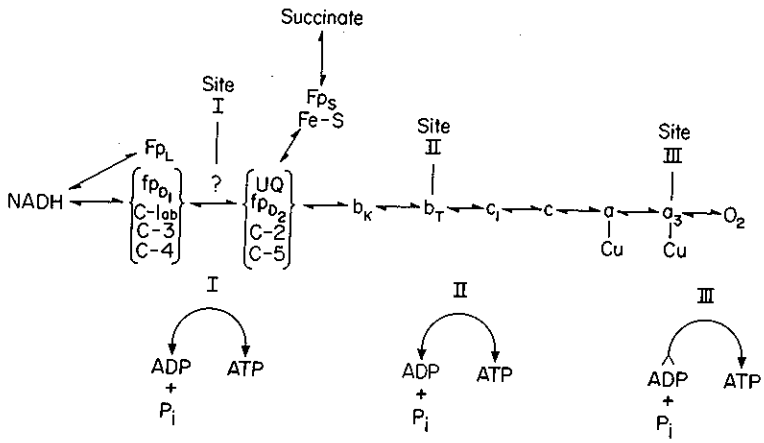

Figure 5. Schematic diagram of the respiratory components from the most negative (NADH) to the most positive (O_2) midpotential.

Figure 6 illustrates the relationship between the percent of maximal NADH oxidation and the corresponding value for cytochrome c in a suspension of rat brain mitochondria. Under these conditions, 50% oxidation of NADH occurs with only 10% oxidation of cytochrome c, as might be expected in view of their relative midpotentials. These levels of oxidation of the two components correspond to about 10^{-7} M oxygen, or 0.07 torr.

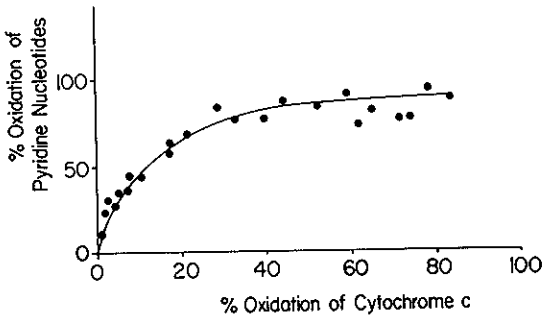

Figure 6. Relationship between extent of NADH oxidation and percent of cytochrome c oxidation, in the former case taken as a fraction of steady state values. Rat brain mitochondria. (TS-N-8A)

Oxygen Requirements for Energy Coupling

It is essential in order to evaluate cell function to know the oxygen concentration at which energy coupling can be activated, and for this purpose we have studied one of the several energy-linked functions of mitochondria (13), the ability of the mitochondria to accumulate divalent cations such as Ca^{++}. This ability is measured with exquisite sensitivity by the jellyfish protein, aequorin (14) kindly provided by Dr. F. H. Johnson. As the mitochondrial suspension is slowly rendered anaerobic, there is an oxygen concentration -- and a corresponding oxidation-reduction level for cytochrome c -- at which aequorin indicates by its luminescence the release of Ca^{++} from the mitochondrial membranes (15). A summary of experimental data for avian cardiac mitochondria is shown in Table I, where both the reduction level of cytochrome c and the corresponding oxygen concentration are listed, together with the number of experiments and the substrate employed. As would be expected, there is some variation with different substrates of the citric acid cycle. In general, however, energy coupling as indicated by Ca^{++} retention, is feasible up to considerable degrees of reduction of cytochrome c.

TABLE I

O_2 Concentration Producing Ca^{++} Release from Mitochondria

		O_2 ($\times 10^{-7}$M)	% Reduction, c
Succinate + Glutamate + Malate	(3)	1.0	66
Succinate + Glutamate	(7)	0.9	70
Glutamate + Malate	(3)	1.1	58
Glutamate	(5)	0.6	47
β-hydroxybutyrate	(2)	0.9	41
Malate	(2)	0.4	75

Thus the oxidation-reduction state of cytochrome c is an effective indicator not only of the electron transport rate through the respiratory chain but also of the capability of the mitochondria for energy coupling. In metabolic state characteristic of living tissues, the graph of Figure 6 gives the appropriate conversion from cytochrome c to NADH oxidation.

SENSITIVE FLUOROMETRY OF TISSUE NADH

Having identified that NADH, being the most sensitive component of the respiratory chain to oxygen, is most competent to serve as an indicator of intracellular oxygen concentrations, and having determined the degree of NADH oxidation required for energy-linked function, we may consider how the oxidation-reduction state of NADH may be measured. This component is, in fact, a natural fluorochrome; excitation in the range 340-370 nm gives rise to fluorescence emission of the reduced form with a peak centered around 450 nm. Figure 7 shows the fluorescence change from the oxidized to the reduced states in a suspension of rat liver mitochondria. Excitation of NADH fluorescence at 340 nm gives an approximately four-fold increase of fluorescence intensity in the transition from the aerobic, substrate-free state to the anaerobic state of the mitochondria.

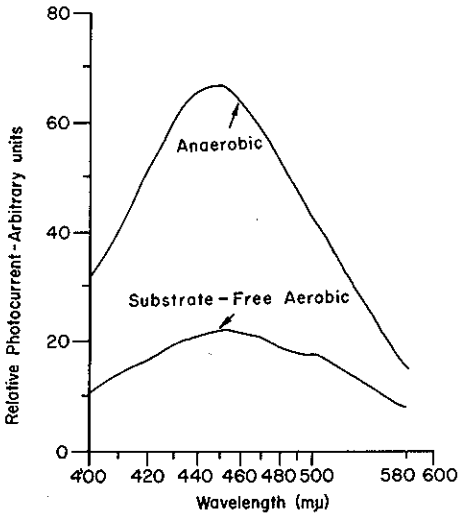

Figure 7. Comparison of the intensity of fluorescence emission from a suspension of mitochondria in the anaerobic vs the aerobic, substrate free states. (Courtesy of The Journal of Biological Chemistry [16]).

This large fluorescence increase may not always be observed in situ, where substrates are continuously supplied to the cell from the bloodstream. Fluorescence increases observed experimentally in living tissue in the normoxic-anoxic transition are in the range of 25% to 50%.

Sensitive fluorometry of tissue NADH has three requirements: 1) a high quantum yield of fluorescence; 2) a high rejection of excitation light from the secondary filter; 3) a control of the magnitude of artifacts due to absorption, reflectance, and scattering changes in the excitation and emission wavelengths.

Quantum Yield

The quantum yield of NADH is relatively low in solution -- approximately 0.1%. Our observations of NADH fluorescence in

the cell, however, indicate that this value is increased by a factor which may run as high as twenty-fold; thus one may expect a quantum yield of approximately 2% for the bound fluorochrome in the tissues. This relatively high quantum yield has three great advantages: first, that of ensuring that NADH will be selectively excited and observed to emit on illuminating the tissue with a wide range of wavelengths in the region from 330 nm to 370 nm; second, that the excitation and emission filters can be relatively simple; third, that artifacts of reflectance and scattering may be minimal.

Filter characteristics

The design of the primary and secondary filters for the measurement of NADH fluorescence involves some fundamental considerations. The first is the choice of wavelengths. 366 nm is appropriate for the excitation of tissue NADH fluorescence and 450 nm for the measurement of its emission for a number of reasons. The absorption of interfering pigments - for example, the difference between the absorption of oxy- and deoxyhemoglobin - dictates this choice of wavelengths. Furthermore, the natural brilliance of the available light sources speaks for the 366 nm bright line of the medium or high pressure mercury arc sources. The sensitivity of photosurfaces is good in the region 440-460 nm.

The monochromatic or broad-band characteristics of the interference or dye filters theoretically speak in favor of the former, but practically in favor of the latter; since the mercury bright line gives essentially monochromatic excitation at 366 nm, the excitation filter does not need to be monochromatic. Interference filters are capable of giving narrow-band response to the emitted light. We have tended, however, to use broad-band filters for emission measurement in order to obtain superior signal-to-noise ratios, although this point may be revised as the techniques for the detection of light signals are further improved.

Absorption, Reflectance, and Scattering Effects

Strong absorption bands of non-fluorescent pigments can imprint their own spectra upon the excitation and emission spectra of fluorochromes and their effects can thereby be readily recognized. In addition, reflectance and light-scattering changes can cause apparent changes of fluorescence intensity, even when the cross between the excitation and emission filters is "perfect" and none of the excitation light directly affects the emission photomultiplier. Reflectance and scattering changes in the sample would, however, have an effect upon both the excitation effectiveness and the emission intensity. For example, increased reflectance of the tissue would decrease the penetration of the exciting wavelength and decrease the observed "fluorescence". Just the opposite effect would be expected with increased light scattering, where the number of interactions of the excitation and emission light-rays with the tissue cells would increase and would therefore enhance the fluorescence emission.

Hemoglobin interference

One of the principal interferences would be expected to be in the oxy-deoxy hemoglobin transition. The spectra of these species for purified hemoglobin is shown in Figure 8, where it is seen that excitation of NADH fluorescence at 366 nm would be subject to an absorption difference in this transition, as would emission at 448 nm.

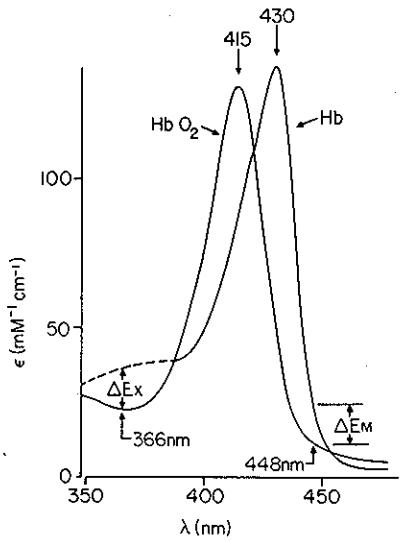

Figure 8. Difference spectrum of oxygenated and deoxygenated hemoglobin, indicating values at which absorption changes are equal and opposite. Thus these wavelengths are suitable for measuring excitation and emission changes. (TA-211).

However, the effects are almost equal and opposite at the two wavelengths; $\Delta Ex \cong -\Delta Em$. Thus, a decrease of absorption of excitation is approximately corrected for by an increase of transmission at the emission wavelength.

Reflectance and emission spectra.

Figure 9 shows the changes of the reflectance spectrum of the rat brain cortex in the aerobic-anaerobic transition (air-nitrogen) in the wavelength region 700-400 nm. Such a curve is of most interest as a "difference" spectrum, since corrections for the properties of the detector are not included. It shows, however, the large change of reflectance in the red region at approximately 625 nm and the isosbestic point near 580 nm. The reflectance in the aerobic tissue in the region of measurement of the fluorescence emission (400-500 nm) is less in air than in the presence of nitrogen. The decrease of absorbancy at 625 nm can, in the air-nitrogen transition, be clearly attributed to hemoglobin (this is the "window" that is traditionally used in ear oximeters). At the shorter wavelengths,

the difference spectrum of oxy-deoxy hemoglobin is small and a generalized scattering change causes increased reflectance of the brain in nitrogen as compared with air.

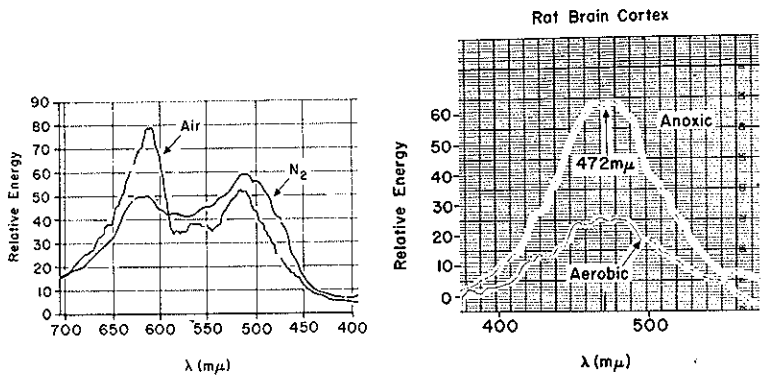

Figure 9. A, reflectance spectra of a normoxic (air) and anoxic (N_2) rat brain cortex observed with a wide spectral interval (~30 nm) and on a relative energy basis, as would be detected by a surface fluorometer. B, fluorescence emission spectra of normoxic and anoxic rat brain cortex observed through a similar optical system with a similar spectral interval. (Courtesy of The Review of Scientific Instruments [17]).

This result is consistent with the fluorescence emission spectrum of the rat brain cortex shown in Figure 9B, obtained with 366 nm excitation. The sharp absorption bands of the hemoglobin-oxyhemoglobin spectrum are not imprinted upon the emission spectra; there is no evidence of the isosbestic points at 445 and 548 nm, or of the absorbancy changes of different sign above and below 445 nm. Thus, the experimental data suggest a relatively minor screening effect of hemoglobin vs. oxyhemoglobin. Figure 9A, however, indicates a reflectance or scattering change that may affect the fluorescence emission measurements in the air-nitrogen transition.

The question of whether or not hemoglobin deoxygenation itself causes a fluorescence emission change is further explored in Figure 10. In this case, a dual wavelength reflectance spectrophotometer has been employed to measure hemoglobin deoxygenation and the usual fluorometer (366 nm excitation, 450 nm measurement) to measure NADH reduction and any associated artifactual response. The experimental procedure is to proceed slowly from normoxia to anoxia so that the tissue passes through a series of steady states in which the hemoglobin and pyridine nucleotide systems may separately reach their appropriate levels as the inspired oxygen is decreased from 20% to 10% to 6% to zero. It is apparent from the record that a 60% deoxygenation of hemoglobin occurs with only a 16% change of the uncorrected fluorescence intensity. Thereafter, the pyridine nucleotide is abruptly

reduced while the remainder of the hemoglobin is deoxygenated. Thus, there is no proportionality between the hemoglobin deoxygenation and the fluorescence increase, as would be expected for pure absorption interference. It is apparent that not only is the effect small, but the choice of a wavelength centered about the isosbestic point for the hemoglobin-oxyhemoglobin transition largely removes the simple absorption difference effect due to the normoxic-anoxic transition.

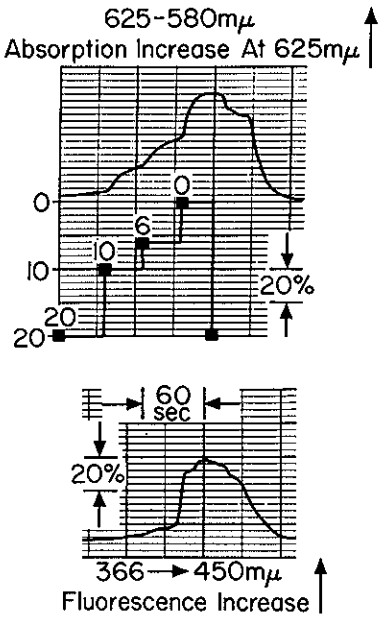

Figure 10. A comparison of the dual wavelength absorbance changes at 625-580 nm and the fluorescence emission changes at 450 nm, in response to 366 nm excitation, as measured on the rat brain cortex through the same optical path and in response to decreases of inspired oxygen of 20%-10%-6%-0.

Simultaneous Recordings of Reflectance and Fluorescence

In order, however, to estimate the reflectance change in a continuous manner during normoxic-anoxic-normoxic cycles, we record a reflectance signal together with the fluorescence emission excited at the same wavelength, as was done some time ago in electric stimulation of slices of the organ of the electric fish in experiments together with R. D. Keynes and X. Aubert (18). Jobsis et al.(19) have used 366 nm as a wavelength for monitoring reflectance for some time while Kobayashi et al. (20) use 620 nm; in the latter case, a computed function of the reflectance was used to correct the fluorescence trace. In this laboratory, Harbig has employed combined reflectance at 366 nm and 450 nm, based upon a modification of the Ultropak apparatus employed by Chance and Schoener (21); these results will appear elsewhere (22). The apparatus described in this and the accompanying paper by Mayevsky and Chance (23) employs reflectance at 366 nm with a linear correction term at 1:1 gain.

The charts illustrate the current state of technology available with a time-sharing fluorometer based upon an air turbine containing the excitation and emission filters. The turbine employed in the

experiments of Figure 11 contains filters appropriate to 366 nm excitation and to reflectance measurements at 366 and 577 nm. The latter wavelength is also employed for excitation of electrochromic probes, results on which are reported elsewhere (24). The fluorescence is picked up by a separate photomultiplier containing a narrow-band secondary filter at 445 nm (as close to the 448 nm wavelength indicated in Figure 9 above as feasible) of 5 nm half-bandwidth in Figure 11A, and in Figure 11B through a broad-band filter combination comprised of a Wratten 47 and a Wratten 2C, which has half-bandwidth points at 420 and 480 nm, with a peak near 450 nm.

The top trace represents reflectance traces similar to those of Figure 3 of the accompanying paper (21) corresponding, in Figure 11A to an "early" reflectance change, and in Figure 11B to somewhat later experiments on the same animal and similar to those of Figure 2, p. 279 . Due to reversed polarity changes in the recorder, the sense of all the traces is opposite to those of the Mayevsky and Chance paper; the time scales, however, and gain calibrations are identical. Thus, the 366 nm reflectance trace (next to the top) shows the characteristic initial decreased reflectance which is coincident with the increase of fluorescence in the uncorrected trace (second from the top). A 1:1 subtration of the two traces gives what is termed the "corrected: fluorescence trace. Additional information is provided by the 577 nm reflectance trace, which changes in the opposite direction from the 366 nm reflectance in the initial phase, but in the same way in the final phase. The sensitivities of all the reflectance and fluorescence traces are the same, and indicated to be 20% for two scale divisions. The next two traces represent the electrocorticogram at a scale of 500 μV, as indicated by the markers.

The experimental traces indicate that the initial decrease of reflectance at 366 nm is simultaneous with the fluorescence increase due to NAD reduction, and thus tends to obscure the initial phases of anoxia as measured on the uncorrected fluorescence trace. However, the late reflectance increase which occurs after the point "SN" (stop nitrogen) is nevertheless prior to the abrupt reoxidation of NAD due to the arrival of oxygen at the brain tissue. It should be noted that this secondary phase of reflectance is almost undetectable in Figure 11B, which represents a recovery from a late anoxia. In either case, the recovery from anoxia occurs at a time when the change of light reflectance at 366 nm is minimal. Observations of isolated mitochondria and perfused organs indicate that the "cycle" of normoxia-anoxia-normoxia is symmetrical, with equal amplitudes in both directions (25). This provides an external control over the efficacy of the compensation procedure by comparing the amplitude of the fluorescence decrease in recovery from anoxia with the fluorescence increase at the onset of anoxia; the two should be identical. Based on observations of perfused organs, a plateau at a constant level of fluorescence should be observed in the interval after reaching the steady state and prior to the recovery from anoxia. It is apparent that the compensated fluorescence traces are consistent with what is known of the performance of isolated organs.

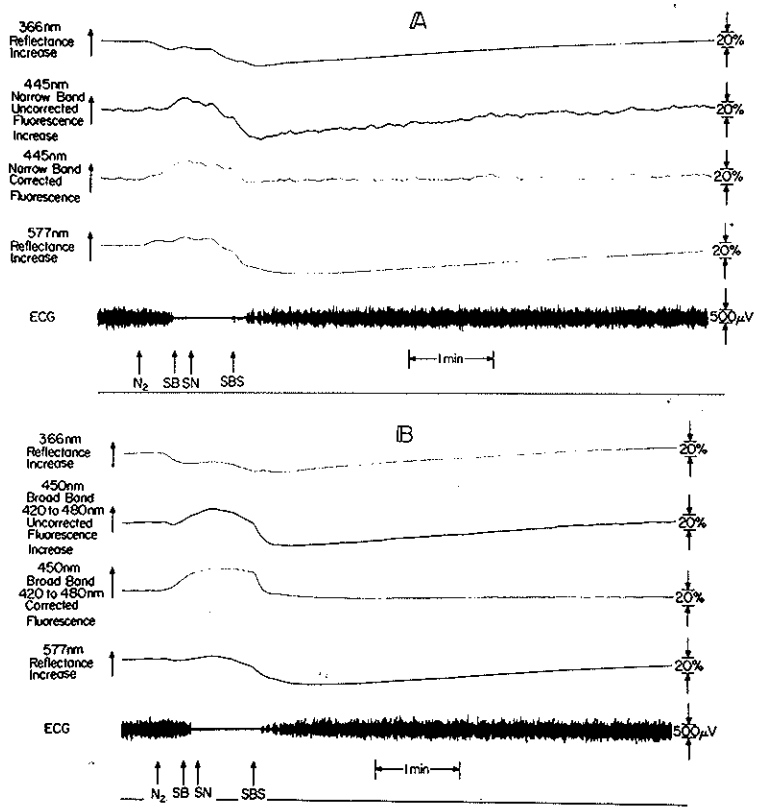

Figure 11. Combined reflectance and fluorescence measurements of the rat brain cortex in cycles of normoxia-anoxia-normoxia. 11A shows results obtained with the narrow-band filter (5 nm half-bandwidth) centered at 445 nm and taken in the early interval of experimentation, i.e., with a fresh animal. 11B represents similar data obtained later in the course of experimentation on the same animal, but employing a wide-band emission filter of half-bandwidth extending from 420 nm to 480 nm, and peaking at 450 nm. The calibrations appropriate to the eight traces are similar, as are the calibrations for the ECG's. Note that increasing intensity is indicated as an upward deflection in this figure, as contrasted with Figures 2 - 4 of the accompanying paper, where increases are indicated as downward deflections. Symbols: N_2, inspiration of 100% nitrogen; SB, stop breathing; SN, stop nitrogen; SBS, start breathing simultaneously.

Lastly, the fluorescence traces compare the responses available with the narrow-band and wide-band filters. Except for the increased noise on the narrow-band trace (A), and the fact that this represents an earlier anoxia than that shown in (B), the corrected traces are identical. We may conclude, therefore, that the wide-band filter simulates the performance of the narrow-band filter by distributing wavelengths on either side of 445 nm to cancel out the hemoglobin changes.

The corrected traces of Figure 11 are similar to those obtained by Chance and Schoener (21, 26) who made most of their observations of NADH kinetics in later cycles of animal study, where the reflectance changes are more of the pattern of Figure 11B. Thus we find confirmation and extension of their results.

DISCUSSION

Precise calibrations of isolated mitochondria for the oxygen requirement for electron transfer and energy coupling (27) indicate that approximately 50% reduction of NAD from the normoxic level corresponds to approximately 10^{-7} M oxygen (0.07 torr), with some variation depending upon the metabolic rate of the tissue. This degree of NAD reduction corresponds to the point at which the mitochondria are no longer capable of energy coupling, as discussed here in terms of their ability to maintain Ca^{++} gradients. Thus, reduction of NAD beyond 50% indicates an insufficiency of oxygen not only for electron transport through the respiratory chain, but for energy coupling as well. In previous work, it was noted that 80-90% reduction of NADH was associated with the cessation of electrical activity as measured by the ECG, and this was identified as a critical pyridine nucleotide reduction (CPNR) (21). It is apparent from the data presented here that the ECG ceases at approximately the same level of NADH fluorescence as that identified in the previous publication (21). Since the mitochondrial calibrations indicate that roughly 50% reduction of NAD from the normoxic level corresponds to the cessation of energy metabolism, we find a close correlation between the *in vitro* data and the *in vivo* data on cessation of the ECG in relation to increased NAD reduction in brain tissue. Presumably the difference between the two values corresponds to the time required for depletion of energy reserves in the brain in terms of creatine phosphate and ATP.

SUMMARY

Problems of precise fluorometry of NADH on the brain cortex have been described, and the conclusions are applied to the design of a time-sharing fluorometer which permits the illumination of the brain with appropriate wavelengths of light, and measurement of both fluorescence emission and reflectance signals via ultraviolet transmitting light guides from the anesthetized animal. This paper examines the appropriateness of these wavelengths and the desirable degree of monochromaticity of both excitation and emission wavelengths and the problem of measuring NADH fluorescence changes in spite of significant changes of absorbancy and reflectance on the

brain cortex during normoxic-anoxic-normoxic cycles. It is concluded that an appropriate choice of wavelengths and spectral intervals substantially removes the absorption of hemoglobin as a disturbing parameter, and leaves mainly reflectance and scattering changes consequent to hemodynamic and cell volume changes in the metabolic transitions. These changes, measured as reflectance on the brain at appropriate wavelengths, are entered as a correction term to the observed fluorescence changes, with the result that normoxic-anoxic-normoxic cycles are obtained which exactly simulate those to be expected on the basis of studies of isolated mitochondria and perfused organs.

The previous conclusion on the correlation between the degree of NAD reduction and the disappearance of the ECG is substantiated and extended by these data, and the critical pyridine nucleotide reduction (CPNR) remains a valid criterion for energy metabolism in the brain cortex. The present data show how these results can be obtained by compensated fluorometry in the fresh animal that exhibits reflectance artifacts in the fluorescence traces. Furthermore, data on isolated mitochondria show that the CPNR level corresponds almost exactly to the degree of anoxia at which the mitochondria are no longer competent in bioenergetic function. The exact pO_2 at which this occurs depends upon the metabolic flux but is generally in the range of 10^{-7} M oxygen or 0.07 torr.

ACKNOWLEDGEMENTS

The authors wish to acknowledge the contributions of Victor Legallais to the mechanical design of the time-sharing units and of Norman Graham, John Sorge, and Michael Mason to the electronic circuitry. They are also grateful for the collaboration of other members of the Johnson Research Foundation and the Department of Neurology, especially Drs. Klaus Harbig, Martin Reivich, and Arisztid Kovach. The research was supported by NINDS-10939-01.

REFERENCES

1. D. W. Bronk. The American Scientist, 34, 55 (1946).
2. P. W. Davies and F. Brink. Rev. Sci. Instr., 13, 524 (1942).
3. P. W. Davies and A. Remond. Res. Publ. Assoc. Res. Nerv. & Ment. Dis., 26 205 (1946).
4. O. Warburg. Heavy Metal Prosthetic Groups and Enzyme Action. (Trans. A. Lawson). Clarendon Press, Oxford, 1949.
5. D. Keilin. The History of Cell Respiration and Cytochrome. Cambridge University Press, Cambridge, 1966.
6. B. Chance and V. Legallais. Rev. Sci. Instr., 30, 732 (1959).
7. B. Chance, R. Perry, L. Åkerman, and B. Thorell. Rev. Sci. Instr., 30, 735 (1959).
8. B. Chance. J. Biol. Chem., 151, 553 (1943).
9. B. Chance and M. Erecinska. Arch. Biochem. Biophys., 143, 675 (1971)
10. F. Schindler. Ph.D. Dissertation, University of Pennsylvania, 1964.

11. R. Oshino, N. Oshino, M. Tamura, L. Kobilinski, and B. Chance. Biochim. Biophys. Acta, 273, 5 (1972).
12. B. Chance and G. R. Williams. J. Biol. Chem., 217, 409 (1955).
13. Energy-Linked Functions of Mitochondria (B. Chance, Ed.) Academic Press, New York, 1963.
14. O. Shimumura, F. H. Johnson, and Y. Saiga. J. Cell. Comp. Physiol., 59, 223 (1962).
15. G. Loschen and B. Chance. Nature New Biology, 233, 273 (1972).
16. B.Chance and H. Baltscheffsky. J. Biol. Chem., 233, 736 (1958).
17. B. Chance, V. Legallais, and B. Schoener. Rev. Sci. Instr., 12, 1307 (1963).
18. X. Aubert, B. Chance, and R. D. Keynes. Proc. Roy. Soc., B-160, 211 (1964).
19. F. F. Jöbsis, M. O'Connor, A. Vitale, and H. Vreman. J. Neurophysiol., 34, 735 (1971).
20. S. Kobayashi, K. Kaede, K. Nishiki, and E. Ogata. J. App. Physiol., 31, 693 (1971).
21. B. Chance, B. Schoener, and F. Schindler. In Oxygen in the Animal Organism (F. Dickens and F. Neil, Eds.) Pergamon Press, Oxford, 1964. p. 367.
22. K. Harbig and M. Reivich. Submitted to J. Appl. Physiol.
23. A. Mayevsky and B. Chance. This Volume, p.239.
24. B. Chance. Proc. Am. Philos. Soc., in press.
25. B. Chance, J. R. Williamson, D. Jamieson, and B. Schoener. Biochem. Z., 341, 357 (1965).
26. B. Chance, P. Cohen, F. Jöbsis, and B. Schoener. Science, 137, 499 (1962).
27. N. Oshino, T. Sugano, R. Oshino, and B. Chance. Federation Proc., 32, 344Abs (1973).